Acceleration of Low-temperature Bainite

C. GARCIA-MATEO, F. G. CABALLERO[1] and H. K. D. H. BHADESHIA

University of Cambridge, Department of Materials Science and Metallurgy, Pembroke Street, Cambridge CB2 3QZ, UK.
1) Centro Nacional de Investigaciones Metalúrgicas (CENIM), Consejo Superior de Investigaciones Cientificas (CSIC), Avda. Gregorio del Amo, 8, 28040 Madrid, Spain.

Recent work has shown that bainitic ferrite plates produced by transformation at low temperatures can be as thin as 20 nm with a hardness in excess of 650 HV. However, it may take several days in order to achieve the required degree of transformation at low temperatures. In this work we report methods for accelerating the rate of reaction without compromising strength.

KEY WORDS: bainite; retained austenite; phase transformations; kinetics.

1. Introduction

It has been discovered that bainite with an ultimate tensile strength in excess of 2.3 GPa and a toughness of some 30 MPa m$^{1/2}$ can be obtained in high-carbon, silicon-rich steels by transformation at homologous temperatures which can be as low as $T/T_m \simeq 0.25$, where T_m is the absolute melting temperature.[1–3] The reported combination of mechanical properties is a consequence of the very thin bainite plates (20–40 nm thickness) and the fine-scale dispersion of austenite between the plates, obtained by transformation at the low temperature. Carbides are avoided in the microstructure by a judicious use of silicon as an alloying element.

In the steel studied, bainite can take between 2 to some 60 d to complete transformation within the temperature range 125–325°C, **Table 1**. A slow transformation at a low temperature (*e.g.*, 200°C, 9 d) is not necessarily a disadvantage since there is no need to cool the sample rapidly to the isothermal transformation temperature. Even a large steel component can therefore reach a homogeneous temperature prior to the onset of transformation, thereby mitigating residual stresses. And a low-temperature heat treatment is not in itself expensive since the energy requirements decrease as the temperature is reduced, and because there is no need to protect the steel against oxidation.

It may nevertheless be useful for small components to be able to accelerate transformation without losing the ability to transform at a low temperature and whilst retaining the fine microstructure which gives the desirable properties. It was the aim of the present work to design alloys which accelerate the formation of bainite at low temperatures.

2. Method

Transformation can be accelerated by increasing the free energy change accompanying the austenite (γ) to ferrite (α) transformation. This has to be done without compromising

the hardenability of the system if other high-temperature phases are to be avoided. It is well known that both cobalt and aluminium increase the free energy change.[4] The basic alloy composition stated in Table 1 was therefore modified to create two further alloys, one containing cobalt and the other a combination of cobalt and aluminium.

It is worth noting that an increase in the driving force at constant temperature may be beneficial in further refining the microstructure in two ways, by promoting the formation of a greater quantity of bainitic ferrite, thereby eliminating islands of retained austenite, which are known to be detrimental to mechanical properties.[5,6] It is the films of austenite between the plates of bainitic ferrite which are desirable. A second advantage could be a refinement of the size of the bainitic ferrite plates themselves, because an increase in the driving force stimulates a greater number density of plates.[7]

Another common method of accelerating transformation is to refine the austenite grain size by using a lower austenitisation temperature or time. This can lead to contradictory effects in the case of the bainite reaction[8]; the reaction can be retarded if the austenite grain boundaries rapidly become saturated with bainite plates, before the sheafs have had a chance to penetrate the grains. This scenario does not apply to the present context where the transformation rate is slow.
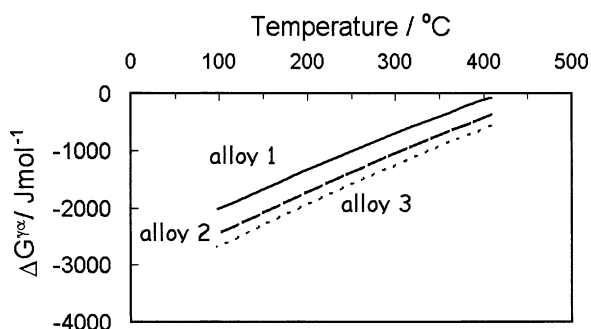
3. Experimental Details

The chemical compositions of the alloys, measured after

Table 1. Chemical composition and measured time (d) required for the bainite reaction to stop.[2]

C	Si	Mn	Mo	Cr	V wt%
0.98	1.46	1.89	0.26	1.26	0.09

125°C	150°C	200°C	250°C	300°C	325°C
>60 days	>30 days	9 days	3–4 days	1–2 days	1–2 days

Table 2. Chemical compositions of experimental alloys, wt%.

Alloy	C	Si	Mn	Mo	Cr	V	Co	Al
1	0.98	1.46	1.89	0.26	1.26	0.09		
2	0.83	1.57	1.98	0.24	1.02		1.54	
3	0.78	1.49	1.95	0.24	0.97		1.60	0.99

Table 3. Measured transformation-start temperatures and austenite grain size, expressed as a mean lineal intercept $\bar{L}_\gamma$ following the stated heat treatment. The uncertainties represent $\pm 1\sigma$.

Alloy	1	2	3
$M_S/°C$	125	120	155
$B_S/°C$	335	360	385
$\bar{L}_\gamma/\mu m$, 1000°C 15 min	49 ± 2	88 ± 4	44 ± 2
$\bar{L}_\gamma/\mu m$, 900°C 30 min		29 ± 2	28 ± 2

Fig. 1. The free energy change $\Delta G^{\gamma\alpha}$ as a function of temperature for the alloys listed in Table 2.

homogenisation at 1 200°C for 2 d whilst sealed in a quartz capsule containing pure argon, are given in **Table 2**.

Calculations of the driving force for the transformation of austenite into ferrite of the same composition, $\Delta G^{\gamma\alpha}$, carried out using MTDATA,[9] confirm the expected[4] effect of cobalt and aluminium on the relative stabilities of austenite and ferrite (**Fig. 1**).

During processing, it is important to ensure that the cooling rate from 1 200°C to ambient temperature is slow enough to avoid martensitic transformation since the high-carbon martensite plates tend to crack spontaneously, permanently compromising the integrity of the sample. The cooling from 1 200°C was therefore accomplished by switching off the furnace to obtain pearlite as the microstructure at ambient temperature.

The procedure for protecting samples against oxidation by sealing in quartz tubes was used for all heat treatments, including austenitisation at 1 000°C for 15 min (or 900°C, 30 min) prior to isothermal transformation at temperatures in the range 125–300°C.

X-ray experiments were conducted using a Phillips PPW1730 diffractometer and a scanning rate (2θ) of $0.1° \min^{-1}$ over the range $2\theta = 30$–$110°$, with unfiltered Cu K_α radiation. The system was operated at 45 kV and 45 mA. The retained austenite content was calculated using integrated intensities of the 111, 200, 220 and 311 austenite peaks and the 110, 002, 112 and 022 peaks of ferrite. Using this number of peaks avoids possible bias due to crystallographic texture.[10] The $\{111\}_\gamma$ and $\{110\}_\alpha$ peaks show some overlap but were separated using Reitveld analysis[11]; the separation is constrained by the information from the other peaks which are isolated.

Specimens for transmission electron microscopy were machined from 3 mm diameter rods which were sliced into 100 μm discs. These were ground down to 50 μm thickness using 1 200 grit silicon carbide paper, for electropolishing at 50 V using a twin-jet unit. The electrolyte consisted of 5% perchloric acid, 15% glycerol and 80% methanol. A JEOL JEM-200CX transmission electron microscope operated at 200 kV was used to examine the thin foils.

Isothermal experiments to measure the bainite-start temperature (B_S) were conducted at 25°C intervals beginning with 250°C and raising the temperature until bainite was not observed over a 24 h period. In some cases, smaller temperature intervals (10°C) were used close to B_S. The highest temperature at which bainite was observed using optical microscopy was designated B_S.

The martensite-start temperatures M_S were determined using 2 mm diameter samples in a high-resolution dilatometer. The samples were heated to 1 000°C and then force cooled using helium at 100 or 200°C s^{-1} to measure the M_S temperature. The results are listed in **Table 3**.

The austenite grain sizes are also presented in Table 3, for two sets of heat treatments. The size was measured by austenitising metallographically polished specimens in a Thermecmastor thermomechanical simulator in a vacuum environment; the resulting thermal grooves revealed the austenite grain structure. Between 60–96 measurements were conducted on optical micrographs taken from the thermally etched samples. Thermodynamic calculations using MTDATA,[9] allowing for the possible existence of cementite, vanadium carbide, austenite and ferrite, confirmed that all the elements are in solid solution in austenite at the austenitising temperatures listed in Table 3.

4. Scale of Microstructure

The general microstructure, consisting of plates of bainitic ferrite and retained austenite, has been reported elsewhere for alloy 1[2,3]; that of the two new alloys is not different other than in scale and phase fractions, as reported here.

Transmission electron microscopy was conducted to determine the true plate-thicknesses t, by measuring the mean lineal intercept $\bar{L}_T = \pi t/2$ in a direction normal to the plate length. The thickness t is related to the mean lineal intercept measured using randomly oriented test lines by the relation $\bar{L} \simeq 2t$,[12,13] but L_T is easier to measure since it is rare in transmission electron micrographs that entire plates of bainite can be imaged. The measured plate thickness t is plotted as a function of transformation temperature in **Fig. 2**; the detailed data are presented in **Table 4**.

Theory indicates that the largest effect on bainite plate thickness is due to the strength of the austenite, the free energy change accompanying transformation and a small independent effect due to transformation temperature.[7] Aluminium does not significantly affect the strength of austenite, causing only a 3 MPa change at ambient temperature, due to 1 wt% of aluminium.[14] Cobalt causes a much smaller change in the lattice parameter of austenite when

compared with aluminium, and has a correspondingly smaller (negligible) effect on the proof strength of austenite.[15,16] Therefore, it is concluded that the observed refinement is a consequence mainly of the effect of cobalt and aluminium, on increasing $|\Delta G^{\gamma\alpha}|$.[7]

It is a feature of any refinement process that the reduction of scale is most difficult when the scale is small—this is because parameters such as the amount of surface per unit volume vary with the inverse of the scale. In alloy 2, which starts off with a coarse plate size following transformation at 300°C, a reduction in the austenite grain size causes t to decrease, presumably because of the greater number density of nucleation sites.

Consistent with the increased driving force in the cobalt and aluminium alloyed steels, the total volume fraction of bainite obtained following prolonged holding at any given temperature has increased (Table 4).

5. Hardness

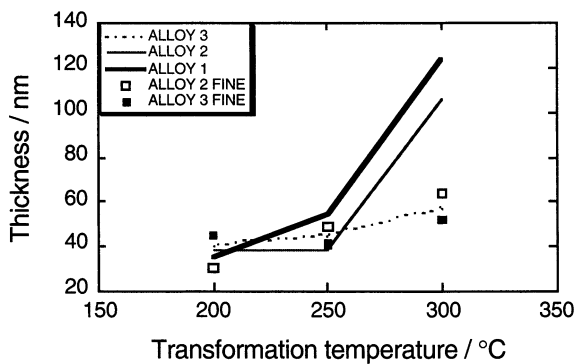The contribution to strength due to the size of the plates is given by $\Delta\sigma = 115(\bar{L})^{-1}$ MPa where $\bar{L}$ is in micrometers.[17–19] From this equation, and given the very fine scale of the bainitic ferrite plate, it is easily shown that much of the strength of low-temperature bainite is due to the fine scale; for example, in alloy 1, $\Delta\sigma \simeq 463$ MPa for plates of thickness 124 nm obtained by transformation at 300°C, whereas $\Delta\sigma \simeq 1642$ MPa for plates of thickness 35 nm obtained by transformation at 200°C.

Since the major strengthening effect is due to the fine plate size, it is expected that the hardness will vary linearly with the reciprocal of the plate thickness, even when other contributions are neglected. The latter include contributions such as solid solution strengthening, variation in the fraction of bainite within the observed range (Table 4) are neglected. The observed trend is consistent with theory, with a correlation coefficient of 0.85 (**Fig. 3**(a)).

In practice, the mean lineal intercept $\bar{L}$ should depend on the fraction of bainite, since the ferrite plates are dispersed in the austenite matrix. Suppose that plates are square with dimensions $t \times a \times a$. The volume per plate would then be ta^2, the number of plates per unit volume $N_V = V_B/ta^2$, where V_B is the fraction of bainite. The surface area per unit volume would thus become

$$S_V = a^2 V_B / ta^2 = V_B / t$$

Since $S_V = 2/\bar{L}$, it follows that the hardness can be related more accurately to the ratio $\bar{L}^{-1} \propto V_B/t$. The hardness is plotted against V_B/t in Fig. 3(b); a slightly higher correlation coefficient of 0.88 is obtained (compared with 0.85, Fig. 3(a)).

6. Rate of Transformation

The two-phase microstructures (austenite and bainitic ferrite) studied here are relatively easy to characterise quantitatively using X-ray diffraction after interrupting isothermal transformation. In particular, martensite (the plates of which are easy to resolve) was never observed after the
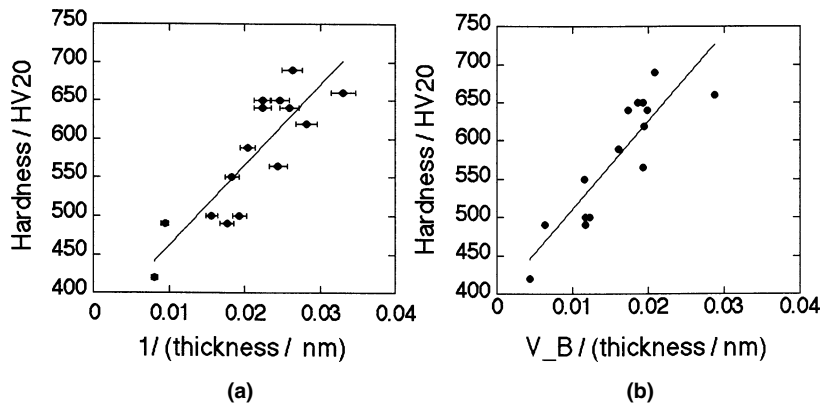

Fig. 2. Plate thickness t as a function of transformation temperature.

Table 4. Summary of quantitative experimental data. V_B designates the fraction of bainitic ferrite, the remainder of the microstructure being retained austenite. The thickness refers to t, the stereologically corrected value. The error is $\pm 1\sigma$ on the thickness. The term 'fine' refers to alloys in which the austenite grain size was refined by austenitising at 900°C for 30 min.

	Temperature / °C	Time /h	Thickness / nm	error / nm	V_B	Hardness / HV20
Alloy 1	300	240	124	4	0.55	420
Alloy 1	250	600	55	1.9	0.63	550
Alloy 1	200	363	35	1.3	0.69	619
Alloy 2 (fine)	300	10	64	3.1	0.75	500
Alloy 2 (fine)	250	14	49	3.2	0.79	589
Alloy 2 (fine)	200	72	30	1.6	0.87	660
Alloy 2	300	24	106	10	0.67	490
Alloy 2	250	24	38	2.5	0.76	640
Alloy 2	200	216	38	2	0.79	690
Alloy 3 (fine)	300	8	52	3.7	0.63	500
Alloy 3 (fine)	250	10	41	1.9	0.79	565
Alloy 3 (fine)	200	72	45	3.3	0.83	650
Alloy 3	300	8	57	4	0.66	490
Alloy 3	250	24	45	3.3	0.77	640
Alloy 3	200	216	40	3.6	0.78	650

Fig. 3. Plot of (a) hardness *versus* the reciprocal of plate thickness; (b) hardness versus V_B/t.
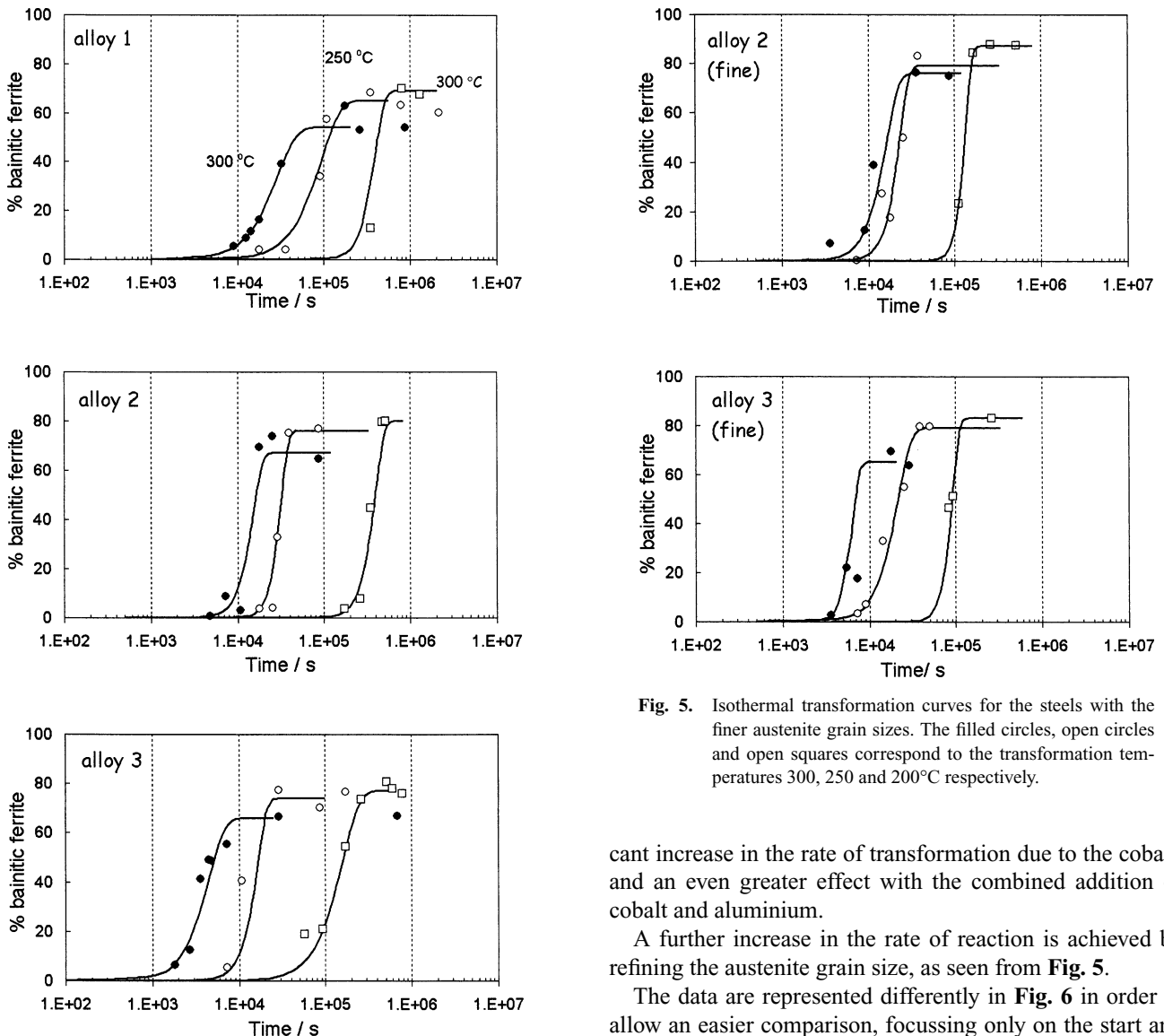

Fig. 4. Isothermal transformation curves. The filled circles, open circles and open squares correspond to the transformation temperatures 300, 250 and 200°C respectively.

Fig. 5. Isothermal transformation curves for the steels with the finer austenite grain sizes. The filled circles, open circles and open squares correspond to the transformation temperatures 300, 250 and 200°C respectively.

cant increase in the rate of transformation due to the cobalt, and an even greater effect with the combined addition of cobalt and aluminium.

A further increase in the rate of reaction is achieved by refining the austenite grain size, as seen from **Fig. 5**.

The data are represented differently in **Fig. 6** in order to allow an easier comparison, focussing only on the start and finish times; the start time corresponds to the first stage at which bainite could be detected using optical microscopy (estimated fraction 0.01), whereas the finish time is when the fraction ceases to change.

onset of the bainite reaction, in any of the samples described below.

The results of an extensive set of experiments like these are illustrated in **Fig. 4**, for alloys 1, 2 and 3, using the high austenitisation temperature. It is clear that there is a signifi-

7. Conclusions

It has been possible to accelerate the bainite transformation at low-temperatures, by adding cobalt and aluminium
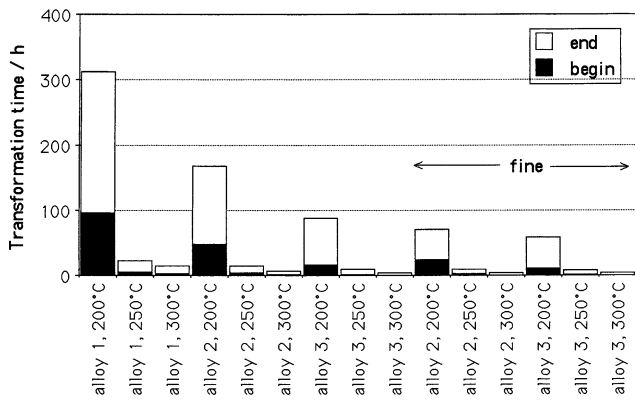
Fig. 6. The reaction start and finish times. The region marked 'fine' refers to samples where the austenite grain size was reduced by using a lower austenitisation temperature of 900°C.

to a high-carbon steel in which the transformation time was originally measured in days. A further acceleration has been obtained by refining the austenite grain size.

The observed effects are attributed to the increase in the free energy change during the transformation of austenite, caused by the alloying additions, and to the increase in the number density of austenite grain surface nucleation sites due to grain refinement.

The modified alloys in general show a more refined microstructure, a greater limiting volume fraction of bainitic ferrite and an increased hardness. All of these effects have been interpreted using the theory of the bainite reaction in steels.

Work is now in progress to characterise the important mechanical properties, including tensile strength, ductility and toughness of these alloys.

Acknowledgments

REFERENCES

1) F. G. Caballero, H. K. D. H. Bhadeshia, K. J. A. Mawella, D. G. Jones and P. Brown: *Mater. Sci. Technol.*, **18** (2002), 279.
2) C. Garcia-Mateo, F. G. Caballero and H. K. D. H. Bhadeshia: *J. Phys. Colloq.*, (2002), accepted for publication.
3) C. Garcia-Mateo, F. G. Caballero and H. K. D. H. Bhadeshia: *ISIJ Int.*, **43** (2003), 1238.
4) H. I. Aaronson, H. A. Domian and G. M. Pound: *Trans. Metall. Soc. AIME*, **236** (1966), 781.
5) H. K. D. H. Bhadeshia and D. V. Edmonds: *Met. Sci.*, **17** (1983), 411.
6) H. K. D. H. Bhadeshia and D. V. Edmonds: *Met. Sci.*, **17** (1983), 420.
7) S. B. Singh and H. K. D. H. Bhadeshia: *Mater. Sci. Eng. A*, **245** (1998), 72.
8) A. Matsuzaki and H. K. D. H. Bhadeshia: *Mater. Sci. Technol.*, **15** (1999), 518.
9) MTDATA: Phase Diagram Calculation Software, National Physical Laboratory, Teddington, UK, (2003).
10) M. J. J. Dickson: *J. Appl. Crystallogr.*, **2** (1969), 176.
11) D. B. Wiles and R. A. Young: *J. Appl. Crystallogr.*, **14** (1981), 149.
12) C. Mack: *Proc. Cambridge Phil. Soc.*, **52** (1956), 246.
13) L.-C. Chang and H. K. D. H. Bhadeshia: *Mater. Sci. Technol.*, **11** (1995), 874.
14) F. Maratray: High Carbon Manganese Austenitic Stainless Steels, International Manganese Institute, Paris, France, (1995), 71.
15) B. Holmes and D. J. Dyson: *J. Iron Steel Inst.*, **208** (1970), 469.
16) F. B. Pickering: *Int. Met. Rev.*, **21** (1976), 227.
17) H. K. D. H. Bhadeshia: Mathematical Modelling of Weld Phenomena III, Institute of Materials, London, (1997), 229.
18) G. Langford and M. Cohen: *Trans. Am. Soc. Met.*, **62** (1969), 623.
19) G. Langford and M. Cohen: *Metall. Trans.*, **1** (1970), 1478.